Proceedings of The National Conference
On Undergraduate Research (NCUR) 2016
University of North Carolina Asheville
Asheville, North Carolina
April 7-9, 2016

Surface Enhancement in Ferroelectric Lithographic Silver Nanowires

Dylan Cromer
Physics
The University of North Carolina at Asheville
One University Heights
Asheville, North Carolina 28804 USA

Faculty Advisor: Dr. James Perkins

Abstract

This paper investigates surface-enhanced Raman spectroscopy (SERS), an important characterization technique with many applications in detection and analysis of trace substances. An electrostatic model of surface enhancement from nano-scale spherical particles is explored, and results from Raman spectroscopy using silver nanoparticles deposited in linear arrays by ferroelectric lithography as SERS substrates are presented. The electrostatic model provides an analytically solved, conceptually simple starting point for SERS theory, whereas fully realistic models must be realized with computational techniques. The experimental results presented show both evidence for and against SERS activity using ferroelectric lithographic substrates. Future theoretical development and experimental work is discussed.

Keywords: Nanoparticles, Raman Spectroscopy, Surface Enhancement

1. Introduction

Raman spectroscopy is a method of characterization which measures the vibrational energy spectrum of a material. Quantized vibrational modes of a molecule can be excited by incident light. Most of these excited molecules fall back to the original level and the light is scattered elastically. Occasionally, however, the vibrational energy falls to a higher or lower level, causing a shift in the light frequency. This process is called Raman scattering. Raman spectroscopy uses these shifts in frequency of the scattered light to detect the vibrational spectrum of the material. A caveat to Raman spectroscopy is that Raman-scattered light is typically weak, making characterization of dilute samples difficult and requiring high intensity light sources. Nearly forty years ago, an effect called surface enhancement was discovered and has since been exploited to amplify Raman-scattered light and expand Raman spectroscopy as a versatile characterization technique.

Surface enhancement is an effect where surface plasmons (quantized electron densities on the surface of conducting materials) oscillate in response to incident electric and magnetic fields, resulting in enhancement of the scattered light. Surface enhancement is a resonance phenomena, occurring at frequencies coinciding with the plasmon resonance frequency, and has only been observed in nano-scale conducting particles. At resonance, the enhancement created has been observed to be up to a factor of 10^6 increase in intensity (see Ref. 6[6]). The plasmon resonance frequency is a function of particle size and shape, which is currently accepted to explain why surface enhancement is only obtainable at optical wavelengths by using nanoparticles.

Surface enhancement can be used for enhancing Raman signals by placing the analyte near the surface of conducting nanoparticles; this technique is called surface-enhanced Raman spectroscopy (SERS). Unlike un-enhanced Raman spectroscopy, SERS is a powerful tool for trace analysis and, as discussed by Haynes, Van Duyne, and McFarland[3], has several applications in biological detection.

Here, ferroelectric lithographic silver nanowires (FLSNs) are discussed as potential SERS substrates. These "wires" are nanoparticles arranged in linear arrays, created by ferroelectric lithography. The technique for growing

FLSNs was first reported by Hanson[2], and was adopted later by Perkins[8], Damm, et al[1], and Molina, et al[5], who demonstrated SERS activity from FLSN substrates.

This paper is organized into two major components. First, the theoretical development of a simple, electrostatic model for surface enhancement effects is presented. This model has been presented by Kelly, et al[4], and Van Duyne, et al[9], and is elaborated here to create a suitable reference for the model at an undergraduate level. Second, FLSNs were grown and tested as SERS substrates. The SERS activity and spatial dependence is specifically examined in the results presented.

2. Theoretical Work

2.1. An Electrostatic Model of Surface Enhancement

Following Kelly, et al[4], the first approach to modeling surface enhancement consisted of considering an isolated silver sphere with dielectric constant ϵ_{in}, placed in some dielectric medium with constant ϵ_{out}, where the incident light subject to the "far-field" approximation. This approximation amounts to the wavelength λ being significantly larger than the particle radius a. With this assumption, the variation of the electric field due to oscillation will be minimal, allowing it to be approximated as a constant and static field, whereas the magnetic field can be treated as negligible. The sphere is placed at the origin, and the electric field is taken to be $\vec{\boldsymbol{E}} = E_0\hat{\boldsymbol{z}}$. Inside and outside of the sphere, the charge density is zero, so in potential form Gauss's law reads

$$\nabla^2 V_{\text{in}} = 0, \tag{2.1}$$

$$\nabla^2 V_{\text{out}} = 0, \tag{2.2}$$

where V_{in} and V_{out} denote the potential inside and outside of the sphere. The potentials are subject to the continuity condition

$$V_{\text{in}}\Big|_{r=a} = V_{\text{out}}\Big|_{r=a}. \tag{2.3}$$

There is a boundary condition at the surface of the sphere,

$$\epsilon_{\text{in}} \frac{\partial V_{\text{in}}}{\partial r}\Big|_{r=a} = \epsilon_{\text{out}} \frac{\partial V_{\text{out}}}{\partial r}\Big|_{r=a}. \tag{2.4}$$

Lastly, the potentials must reduce to the potential for the background field in the $r \to \infty$ limit:

$$V_{\text{out}}(x, y, z) = -E_0 z, \tag{2.5}$$

or in spherical coordinates,

$$V_{\text{out}}(r \to \infty, \theta, \phi) = -E_0 r\cos\theta. \tag{2.6}$$

These equations constitute a complete boundary value problem. The solutions to $\nabla^2 V = 0$ are known and consist of angular dependence in the form of Legendre polynomials in $\cos\theta$ and radial dependence in powers of r:

$$V_{\text{in}} = \sum_{\ell} c_\ell r^\ell P_\ell(\cos\theta), \tag{2.7}$$

$$V_{\text{out}} = \sum_{\ell} d_\ell \frac{1}{r^{\ell+1}} P_\ell(\cos\theta) - E_0 r\cos\theta, \tag{2.8}$$

where P_ℓ are Legendre polynomials, c_ℓ and d_ℓ are constants, and term subtracted from V_{out} is to ensure that the boundary condition at $r = \infty$ is satisfied. These equations were solved by hand, showing that the potential is actually just a single term in the sum, $\ell = 1$, while all other terms are zero. The potential's gradient then gives the full electric field:

$$\boldsymbol{E}_{\text{out}}(r, \theta) = E_0\hat{\boldsymbol{z}} + ga^3 E_0 \frac{1}{r^3}\Big(\frac{3z\boldsymbol{r}}{r^2} - \hat{\boldsymbol{z}}\Big), \tag{2.9}$$

where the factor g contains all dependence on the dielectric media:

$$g = \frac{\epsilon_{\text{in}} - \epsilon_{\text{out}}}{\epsilon_{\text{in}} + 2\epsilon_{\text{out}}}. \tag{2.10}$$

Now that the electric field has been found, it can be calculated near the sphere, given specific dielectric constants for the silver and the exterior material (in this case, water). These constants are complex, with both a real and imaginary part. A list of values obtained from Palik's book[7] is used to make a fit, which approximates the *complex dielectric function* for silver. These constants generally depend on the wavelength of the light, and so the entire electric field becomes a function of the wavelength as well. Given a chosen wavelength, contours of the field strength near the surface of the sphere can be calculated with Mathematica, as shown in Figure 1 for 360 nm, with a sphere size of 35 nm. These are plotted in the yz plane.

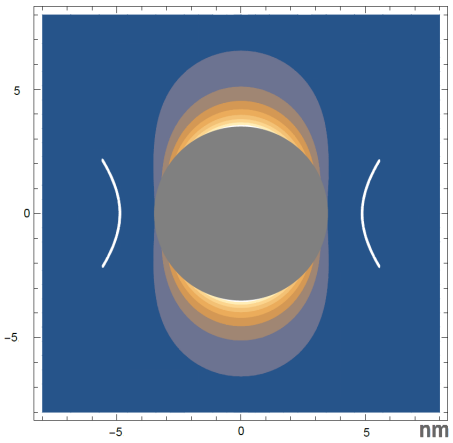

Figure 1: Electric field magnitude contours in the yz plane, with wavelength of $360nm$ and particle radius of 35 nm. The grey circle indicates the interior of the particle. The white semi-circular curves are believed to be numerical artifacts.

This plot shows that the electric field is much like that of a dipole. The field is highly enhanced near the poles. While the field was calculated for a static case, it was approximating a light source whose field will slowly oscillate. This oscillation will result in an oscillation of the poles, which causes enhancement of the light through dipole radiation.

This mechanism would create further enhancement if multiple particles were used; by placing the particles in a line along the polarization direction, the poles of each particle would attract additional charges, polarizing the particle more than in the single-particle case.

2.2. Limitations of the Electrostatic Model

The far-field approximation to the electric field is not useful for creating realistic models of surface enhancement from FLSNs used in the experimental work described in Section 3, as a typical particle size is $10 - 100$ nm, and the incident light wavelength is 532 nm. Since one wavelength is the scale over which one oscillation of the field occurs, this means that the field varies approximately by between $1/50$ and $1/5$ of a cycle over the diameter of one particle. This is at the border of where the constant field approximation is useful. In addition, the typical spacing of the nanoparticles is smaller than the typical diameter of each nanoparticle, and single-particle approximations are hence of limited usefulness. Rather than offer realistic depiction of the behavior of FLSN under Raman spectroscopy, the electrostatic model is useful for understanding the simplest mechanism of surface enhancement at an elementary level.

The electrostatic model offers one surprising result; due to the wavelength dependence of the factor g in equation (2.8), the electric field is itself a function of wavelength. Using a particle size of 35 nm, the electric field contours suddenly change behavior at a wavelength of 350 nm, as shown in Figure 2.

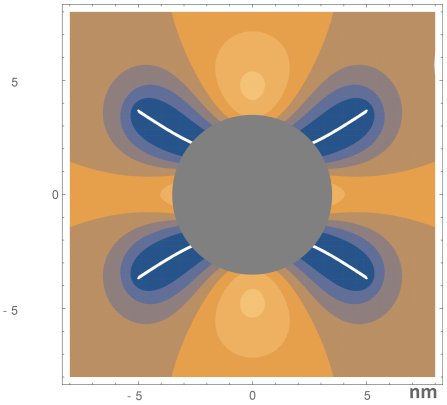

Figure 2: Electric field strength contours with an incident wavelength of 350 nm, and a particle radius of 35 nm. The electric field appears to have a nonzero quadrupole moment.

The electric field now appears to contain a quadrupole moment, rather than consisting purely of a dipole. This behavior is unexpected, and is a result of the complex value of the dielectric function.

3. Experimental Work

3.1. Silver Nanowire Lithography

Ferroelectric lithographic silver nanowires were deposited according to the methods used by Hanson, et al[2]; UV light was used to photoreduce $AgNO_3$ onto periodically poled lithium niobate (PPLN) substrates. PPLN, a ferroelectric substance, has positive and negative electrical domains. Due to the electric field created by these domains, silver nanoparticles form preferentially at the domain boundaries, creating a periodic linear array. This process can be adjusted to control nanoparticle characteristics. This is demonstrated in Figure 3, where scanning electron microscope (SEM) images of two FLSN samples are shown. These samples were created with different growth parameters: the wires on the left were photoreduced for ten minutes using 10^{-4} molar $AgNO_3$, at a fixed distance from the UV light source, and the wires on the right were created with a five minute deposition, and $0.5 \times 10^{-4} M$ $AgNO_3$. This difference in deposition times and solution concentrations resulted in larger average particle size for the left sample, as seen using SEM imaging.

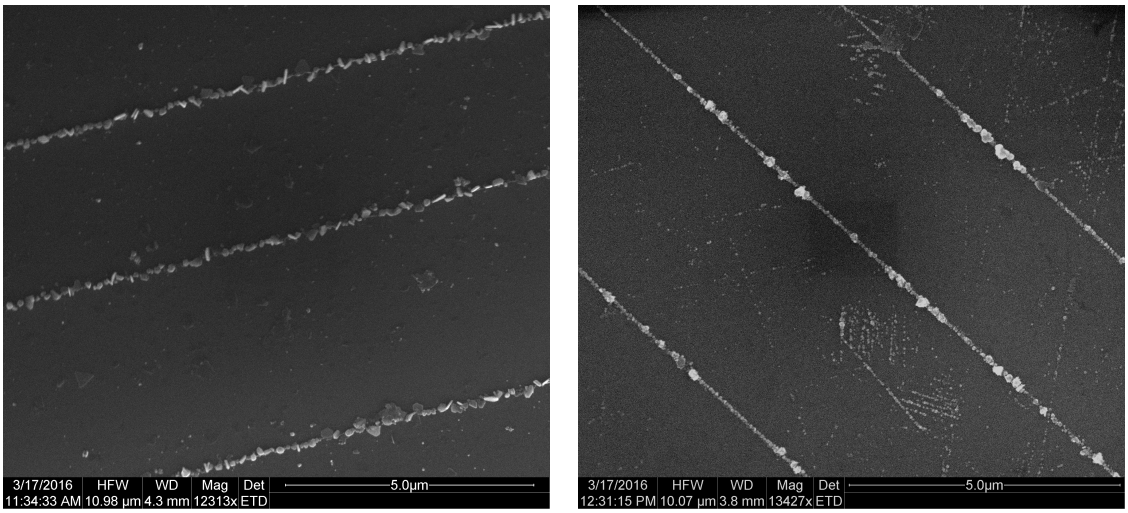

Figure 3: SEM images of two PPLN substrates with FLSNs. The left sample was created with a 10-minute photoreduction, using $1 \times 10^{-4} M$ silver nitrate solution. The sample on the right was deposited for five minutes using $0.5 \times 10^{-4} M$ $AgNO_3$.

3.2. Raman Spectroscopy

Several experiments were conducted to test the SERS activity of FLSNs and spatial dependence of the signal. For these tests, a *BaySpec* $532\ nm$ Raman microspectrometer was used with a $60\times$ objective. In all experiments, the PPLN substrate was placed beneath the microscope objective and a drop of the analyte was put on the substrate surface.

3.2.1. evidence for enhancement effects

One of the first tasks carried out was to obtain a direct comparison between a Raman analyte viewed without any FLSNs on the substrate and viewed with FLSNs. For this purpose, a $4.9 \times 10^{-2} M$ concentration of pyridine was used as the analyte. One set of Raman spectra were obtained by placing this analyte on a PPLN substrate which had no FLSNs. This "clean" sample produced a high-intensity lithium niobate spectrum, but no pyridine spectrum was observable above background levels. One such spectrum is pictured in Figure 4 below.

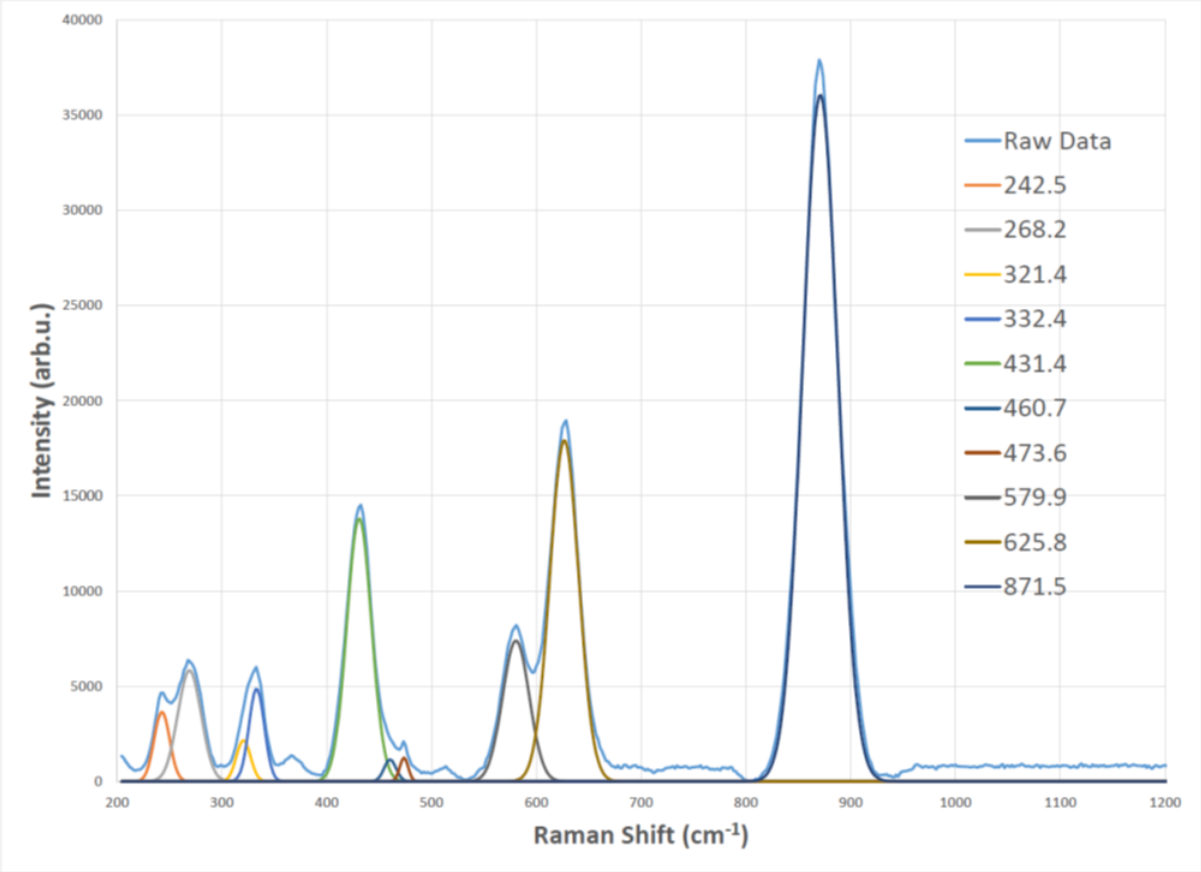

Figure 4: Raman spectrum of $4.9 \times 10^{-2} M$ pyridine on a PPLN substrate without FLSNs, showing lithium niobate peaks.

A further set of spectra was then obtained using the same PPLN substrate, but after deposition of FLSNs, using ten minutes of photoreduction of $1.0 \times 10^{-4} M$ silver nitrate. Again, $4.9 \times 10^{-2} M$ pyridine was used as the analyte. These samples produced a pyridine spectrum which is identifiable, though much weaker than the lithium niobate spectrum. One of these spectra is shown in Figure 5. These results suggest apparent enhancement effects from the presence of the FLSNs.

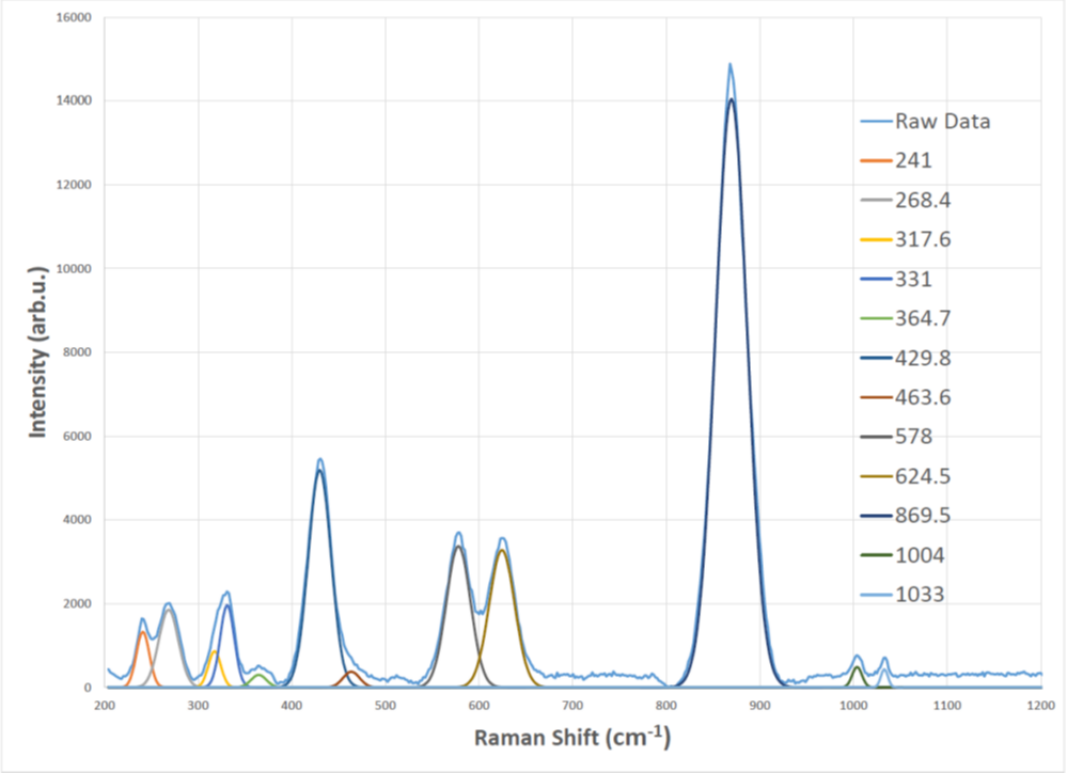

Figure 5: Raman spectrum of $4.9 \times 10^{-2} M$ pyridine on a PPLN substrate with FLSNs, with both lithium niobate and pyridine spectra visible. The pyridine spectrum is the small doublet near 1000 cm^{-1}.

3.2.2. testing spatial dependence

A further method for testing enhancement effects of FLSNs is the measurement of spatial dependence in the Raman signal. Spatial dependence would not only be strong evidence for SERS-active FLSNs, but would also allow the effects of different surface geometries to be tested. A preliminary experiment was devised in which a substrate with FLSNs was translated using precision actuators in steps of 1 μm under the Raman microscope objective. A $2.0 \times 10^{-2} M$ solution of pyridine was used as an analyte and the translations were made perpendicular to the lengths of the FLSNs. For each of these translations, the intensity of the 1000 cm^{-1} pyridine peak was recorded and are plotted below in Figure 6 as a function of displacement.

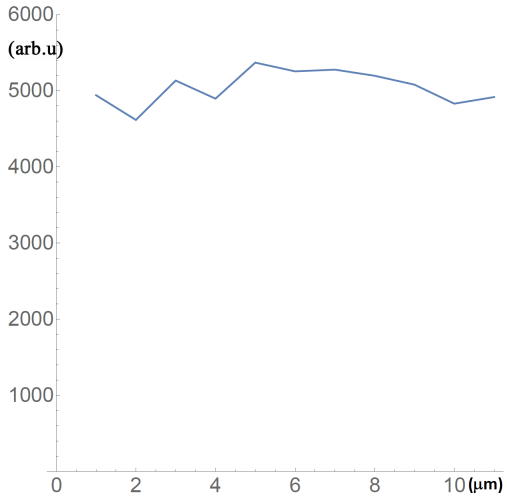

Figure 6: Plot of the intensity of the 1000 cm^{-1} pyridine peak vs. distance translated. Each step on the graph is a distance of 1 μm perpendicular to the linear arrays of FLSNs on the substrate.

The variations are much lower than those expected if SERS effects are both present and spatially dependent.

3.2.3. evidence against enhancement

Another experiment was devised to further test enhancement from the presence of FLSNs by placing FLSNs on only half of a PPLN substrate. These FLSNs were deposited for five minutes using $0.5 \times 10^{-4} M$ silver nitrate. SEM images were used to confirm that the cover substrate successfully prevented FLSNs from depositing on one half of the sample. Three images are shown below in Figure 7. Figure 7 a) shows the covered side, displaying no FLSNs. Figure 7 c) is of the uncovered side, where FLSNs clearly formed. While most of the covered side was free of silver deposition, there were small regions near the borders with very small FLSNs, such as the region shown in Figure 7 b).

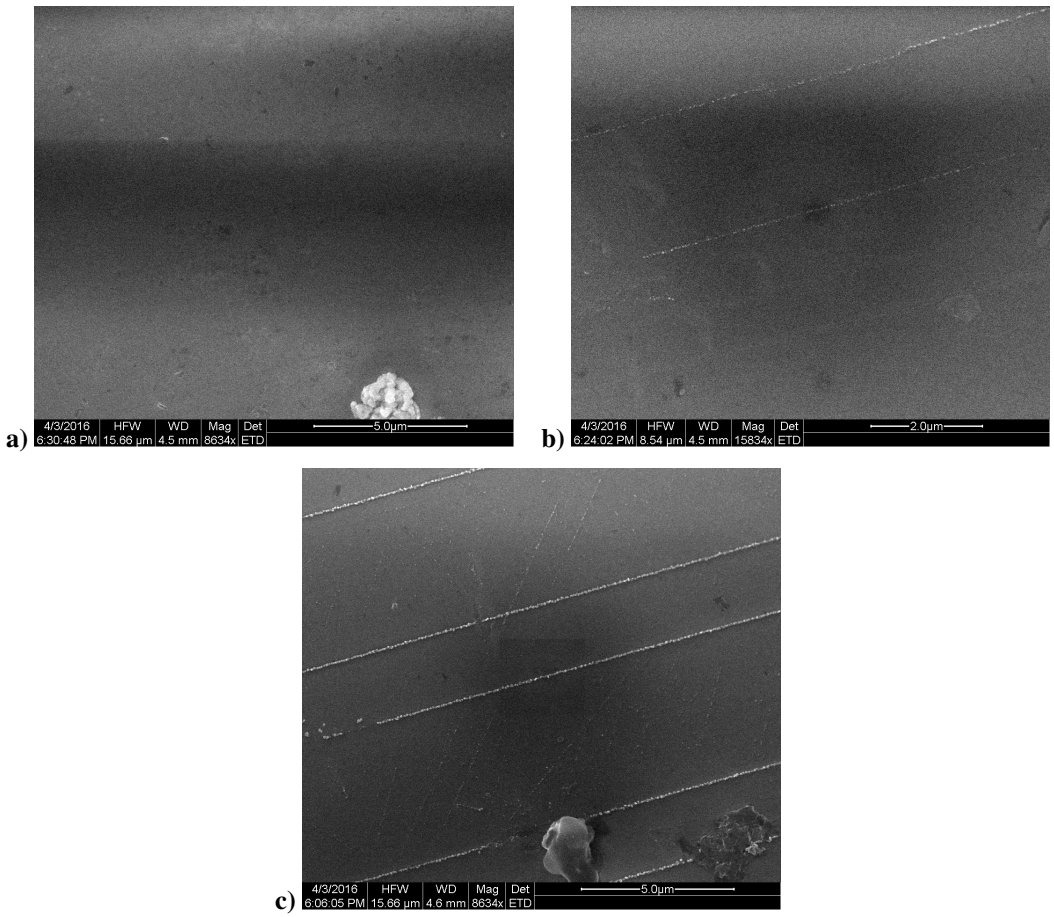

Figure 7: SEM images of the half-covered PPLN substrate after deposition. Images a) and b) show the covered side, and c) shows the uncovered side. The particulate in a) is believed to be dust, and the irregularities in c) are likely scratches on the substrate.

This sample was then used as a Raman substrate, with a $1 \times 10^{-1} M$ pyridine analyte. Raman spectra of the pyridine from each side were obtained, showing almost identical intensities, as shown in Figure 8, where the spectrum from the FLSN-present side is shown in blue, and the FLSN-absent side in yellow.

A further set of spectra were taken without any analyte and only the lithium niobate spectrum was observed, again on both ends of the substrate. Two of these spectra are depicted in Figure 9, again with blue indicating the side with FLSNs and yellow indicating the side without FLSNs. Surprisingly, the spectra show that the side with no FLSNs has approximately double the intensity of the FLSN side.

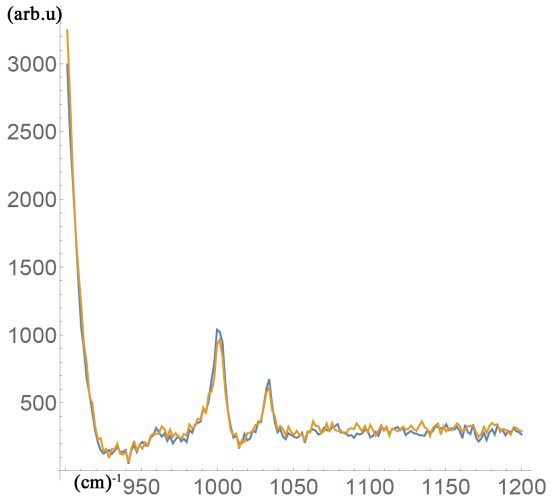

Figure 8: Comparison of the FLSN-present Raman spectrum (in blue) and the FLSN-absent spectrum (in yellow), showing the two pyridine peaks from a $1 \times 10^{-1} M$ pyridine analyte.

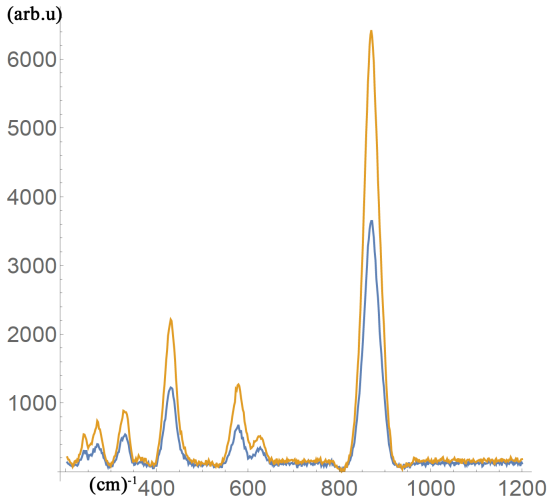

Figure 9: Comparison of FLSN-present(blue)/absent(yellow) Raman spectra with no analyte present, showing only the lithium niobate peaks.

This data suggests, contrary to the data shown in Section 3.2.1, that these FLSNs are not SERS active. Using the larger pyridine peak at 1000 cm^{-1} for a simple estimate on any enhancement of the signal, the ratio of the two signals is

$$\frac{I_{FLSN}}{I_0} = 1.08 \tag{3.1}$$

(where I_{FLSN} is the intensity of the FLSN-present spectrum, and I_0 is the other spectrum intensity), much lower than the usually given 10^6 enhancement factor. The backgrounds on these spectra vary on the order of ± 50 $arbu$ (arbitrary intensity units), which can be taken as the noise level. If this is treated as the uncertainty of the measurement, then the uncertainty of the intensity ratio can be calculated to be ± 0.07 $arbu$. Thus, the factor of enhancement is barely outside of the uncertainty range. This is mitigated by the fact that *both* pyridine peaks have approximately the same intensity ratios, making it less likely that the intensity difference is simply noise. However, given the small magnitude of enhancement, it is more likely that it is due to changes in surface topography altering the focus than due to surface enhancement from FLSNs.

4. Conclusions and Future Work

From the theoretical discussion in Section 2, it is clear that electrodynamic models are necessary to accurately model FLSN SERS activity. It is very likely that computational methods will be needed to solve such models, and

thus future theoretical work will be directed to utilizing computational electrodynamics.

The experimental data obtained suggest that at best, FLSNs are not consistently producing SERS effects under the current setup. There are several possibilities for the source of this problem: the Raman microscope objective has a large depth of focus and may not be confocal. Furthermore, Perkins[8] used laser wavelengths of $479\ nm$, $488\ nm$, and $514\ nm$, whereas the wavelength used here was $532\ nm$. Since SERS is based on resonance, it is possible that FLSNs typically have a plasmon resonance frequency which is closer to the wavelengths used by Perkins, and $532\ nm$ is not sufficiently close to produce enhancement. SERS activity is notoriously hard to reproduce (see Perkins[8]), so it is not known which of these issues, if any, contributed to the difficulty in producing SERS effects.

Future theoretical work may shed light on the problem, as knowing an accurate estimate of the expected spatial dependence of enhancement will aid in designing further laboratory tests. Progress in this area will be immensely useful for improving the reproduction of consistently SERS-active substrates, facilitating the expanded use of SERS as a highly sensitive characterization technique.

5. Acknowledgments

The author would like to thank Dr. James Perkins, the Surfaces, Materials, and Lithography Lab Group at UNC Asheville, the UNC Asheville Physics Department, and the NC Space Grant Consortium. Each party above has contributed towards this work.

6. References

[1] Damm, S., Carville, N. C., Rodriguez, B. J., Manzo, M., Gallo, K., and Rice, J. H., J. Phys. Chem. C **116**, 26543 (2012).

[2] Hanson, J. N., Rodriguez, B. J., Nemanich, R. J., and Gruverman, A., IOP Pub. Ltd **17**, 4946 (2006).

[3] Haynes, C. L., McFarland, A. D., and Van Duyne, R. P., An. Chem. **77**, 338 A (2005).

[4] Kelly, K. L., Coronado, E., Lin Zhao, L., and Schatz, G. C., J. Phys. Chem. **107**, 668 (2003).

[5] Molina, P., Yraola, E., Ramírez, M. O., Plaza, J. L., de las Heras, C., and Bausá, L. E., Nano Lett. **13**, 4931 (2013).

[6] Moskovits, M., Rev. Mod. Phys. **57**, 783 (1985).

[7] Palik, E. D., *Handbook of Optical Constants of Solids* (Academic Press, 1997).

[8] Perkins, J., *Raman Spectroscopy - in situ Characterization of Growth and Surface Processes*, Ph.D. thesis, North Carolina State University (2007).

[9] Stiles, P. L., Dieringer, J. A., Shah, N. C., and Van Duyne, R. P., Ann. Rev. An. Chem. **1**, 601 (2008).